

Quantitative 3D Telomeric Imaging of Buccal Cells Reveals Alzheimer's Disease-Specific Signatures

Angeles Garcia^b, Shubha Mathur^a, Maria Carmela Kalaw^a, Elizabeth McAvoy^b, James Anderson^b, Angela Luedke^b, Justine Itorralba^b and Sabine Mai^{a,*}

^aManitoba Institute of Cell Biology, The University of Manitoba, CancerCare Manitoba, Winnipeg, MB, Canada

^bDepartment of Medicine (Geriatrics) and Neuroscience Centre, Queen's University, Kingston, ON, Canada

Accepted 26 February 2017

Abstract. This study validates and expands on our previous work that assessed three-dimensional (3D) nuclear telomere profiling in buccal cells of Alzheimer's disease (AD) patients and non-AD controls (Mathur et al., *J Alzheimers Dis* 39, 35–48, 2014). While the previous study used age- and gender-matched caregiver controls, the current study consented a new cohort of 44 age- and gender-matched healthy non-caregiver controls and 44 AD study participants. 3D telomeric profiles of buccal cells of AD patients and their non-AD controls were examined with participant information blinded to the analysis. In agreement with our previous study, we demonstrate that 3D telomeric profiles allow for the distinction between AD and non-AD individuals. This validation cohort provides an indication that the total number of 3D telomeric signals and their telomere lengths may be a suitable biomarker to differentiate between AD and non-AD and between mild, moderate, and severe AD. Further studies with larger sample sizes are required to move this technology further toward the clinic.

Keywords: Alzheimer's disease, buccal cells, telomeres

INTRODUCTION

Alzheimer's disease (AD) is the most common form of dementia affecting approximately five million Americans age 65 and older, as well as an estimated 200,000 Americans under the age of 65 who are afflicted with early-onset AD [1, 2]. AD is clinically defined as a progressive neurodegenerative disorder that involves cognitive impairment, memory loss, visual-spatial retrogression, and language impairment [3].

Current guidelines set by the Alzheimer's Association and the National Institute of Neurological

Disorders and Stroke identify three stages of AD: preclinical AD, mild cognitive impairment (MCI) due to AD, and dementia due to AD [4–6]. Every year, approximately 15% of MCI patients progress to dementia [1, 7, 8]. The final stage, dementia due to AD, can be described as a state that affects memory, thinking, and behavior, thus impairing everyday living of a patient, in addition to significant changes in the brain, cerebrospinal fluid, and blood [9]. Dementia due to AD is the most common and most identifiable stage of this condition [9]. In this study, we categorized patients into three stages of mild, moderate, and severe AD based on the patient's cognitive scores on MMSE and MoCA examinations [10–12].

Currently, AD is only confirmed postmortem through pathological studies of the brain and consequently, it is the fifth leading cause of death for people age 65 and older [1, 13]. Although AD has

*Correspondence to: Sabine Mai, Manitoba Institute of Cell Biology, The University of Manitoba, CancerCare Manitoba, 675 McDermot Ave, Winnipeg, MB, R3E 0V9, Canada. Tel.: +1 204 787 2135; FAX: +1 204 787 2190; E-mail: sabine.mai@umanitoba.ca.

been associated with pathologies such as tau protein hyperphosphorylation and amyloid- β (A β) plaque formation, measuring levels of these proteins in the cerebrospinal fluid and blood are not highly specific, and can be invasive [1, 9]. Thus, there is a need for a non-invasive biomarker with high sensitivity/specificity that can diagnose AD and indicate disease progression. In addition to tau and A β pathology, AD has also been correlated with markers of genomic instability such as changes in nuclear telomere length [14–18]. A recent meta-study confirmed telomere shortening in AD [19].

Telomeres are highly repetitive (TTAGGG)_n hexanucleotide sequences situated at the terminal ends of mammalian chromosomes [20–22]. Together with a protein complex termed shelterin, they protect the ends of chromosomes from deterioration and prevent end-to-end fusions with neighboring chromosomes [23]. Telomeres play a vital role in genomic stability and cell senescence, thus making them an important structure in diseases related to genomic instability and aging, including AD [14, 24–27]. Telomeres of normal cells shorten with each cell division until a final critical length is reached; this final critical length is known as the Hayflick limit [28]. At this point of their cell division cycles, normal cells enter a state of senescence, which is considered a tumor preventative state [29]. During senescence, telomeres form aggregates as reported in culture for mesenchymal stem cells [30]. Telomeres were implicated in the age-related deterioration of hematopoietic stem cells [31]. In line with these observations, oncogene-induced escape from senescence was shown to be associated with derepressed hTERT promoter activity [32]. Changes in telomere biology were recently proposed as possible markers for aging [33], and a recent meta-analysis confirmed the loss of telomere sequences as a feature associated with AD [19]. Thus, telomeres may serve as a biomarker for disease including as aging [34] and cancer [35].

The primary objective of this study was to validate the data on changes in the 3D organization of telomeres in AD as reported in a previous AD/non-AD cohort [28]. In this cohort, we described a non-invasive method to examine and define alterations in AD and during AD progression using quantitative 3D nuclear telomere imaging of buccal cells (BCs). As a follow-up to our initial cohort of 82 subjects with age- and gender-matched caregiver controls (41 AD and 41 non-AD) [36], the current study reports on a second independent patient cohort in which we investigated the 3D nuclear telomeric profiles from BCs of 88 study participants using age- and gender-matched non-caregiver controls (44 AD and 44 non-AD). This is in contrast to the previous study that was based on caregiver controls [28]. Our data indicate that 3D telomere lengths and telomere numbers are sufficient to distinguish between AD and non-AD independent of the control group (caregivers or non-caregivers) and between mild, moderate and severe AD.

MATERIALS AND METHODS

Study population

The patients recruited for the study were from Queen's University Memory Clinics and were diagnosed according to the National Institute of Neurological and Communicative Disorders and Stroke, and the Alzheimer's Disease and Related Disorders Association (NINCDS-ADRDA) criteria [3–5]. In total, our study followed 44 AD patients who were age- and sex-matched to 44 normal study participants (Table 1). All AD patients were on standard AD treatment with cholinesterase inhibitors.

The stratification of AD patients as mild, moderate, or advanced AD was based on their regular clinic appointments and their respective Montreal Cognitive Assessment (MoCA) score and the Mini-Mental

Table 1
Patient demographics

Population	Test Score Ranges (MoCA/30;MMSE/30)	Number of Subjects	Mean Age (y \pm S.D)	Gender (Male/Female)
Mild AD	>18: \geq 22	24	76.8 \pm 9.3	6/17
Controls, Mild AD	N/A	24	75.2 \pm 9.9	6/17
Moderate AD	\leq 18:21–16	15	75.8 \pm 9.3	7/8
Controls, Moderate AD	N/A	15	74.5 \pm 7.6	7/8
Severe AD	----: <16	5	85.2 \pm 1.6	2/3
Controls, Severe AD	N/A	5	83.2 \pm 2.5	2/3

AD, Alzheimer's disease; MoCA, Montreal Cognitive Assessment; MMSE, Mini-Mental State Examination. All patients were on treatment with cholinesterase inhibitors.

State Examination (MMSE) evaluations [10–12]. Patients with a MoCA score of $>18/30$ and/or MMSE score of $\geq 22/30$ were considered to have mild AD. Patients with a MoCA score of $\leq 18/30$ and/or MMSE score between 21/30 and 16/30 were considered to be in the moderate stage of AD. Finally, patients with an MMSE score lower than 16/30 were considered to have severe AD. In this study that was performed in a blinded manner, no other classification of AD was done, and no information on disease duration or comorbidities was available.

Collection of buccal cells and sample preparation

The collection of patient samples was done as previously described [36]. Using Epicentre Catch-A11 sample collection swabs, buccal cells were collected by the Queen's University Memory Clinics' personnel in duplicates from each participant's cheek and smeared onto a marked square of microscope VWR pre-cleaned frosted slides. The slides were frozen at -20°C and shipped to the University of Manitoba in dry ice. The Manitoba laboratory personnel were blinded to sample diagnoses, which were revealed upon completion of sample imaging and analysis.

Three-dimensional quantitative fluorescent in situ hybridization of telomeres (3D Q-FISH)

3D Q-FISH was carried out as follows: Slides were fixed using fresh 3.7% formaldehyde/1× phosphate buffered saline buffer (PBS) (formaldehyde, Sigma-Aldrich, St. Louis, MO; Sodium chloride (NaCl), EM Science, Darmstadt, Germany; Potassium chloride (KCl), Fisher Scientific, Fair Lawn, NJ; Sodium phosphate (Na_2HPO_4), Fisher Scientific; Potassium phosphate (KH_2PO_4), Sigma-Aldrich) for 20 min and washed in 1× PBS (NaCl, EM Science; KCl, Fisher Scientific; Na_2HPO_4 , Fisher Scientific; KH_2PO_4 , Sigma-Aldrich) three times for 5 min each cycle. Slides were then incubated in 0.5% Triton X-100 (Sigma-Aldrich) for 10 min, followed by incubation in 20% glycerol (Sigma-Aldrich) for 60 min. Four repeated cycles of a glycerol/liquid nitrogen freeze-thaw treatment were performed. Afterwards, the slides underwent three 1× PBS washes for 5 min each cycle. The slides were then incubated in 0.1 M hydrochloric acid (HCl) (Sigma-Aldrich) for 5 min and 15 s followed by two washes of 5 min in 1× PBS. After equilibration at room temperature for 1–2 h in 70% Formamide/2× saline-sodium citrate

buffer (SSC) (Formamide, Sigma-Aldrich; NaCl, EM Science; Sodium citrate ($\text{NaH}_2\text{C}_6\text{H}_5\text{O}_7$), Fisher Scientific) at pH 7.0, slides were washed twice for 5 min in 1× PBS, and thereafter hybridized with four μl of telomere peptide nucleic acid (PNA) probe (DAKO, Glostrup, Denmark) using a HybriteTM (Vysis, Abbott Diagnostics, Des Plaines, IL). The samples underwent denaturation for 3 min at 80°C , followed by probe annealing to the template for 2 h at 30°C . Slides then underwent a series of washes in 70% Formamide/10 mM Tris at pH 7.4 (Formamide, Sigma-Aldrich; Tris, Sigma-Aldrich) three times for 15 min each cycle, 1× PBS one cycle for 1 min, 0.1× SSC at 55°C one cycle for 5 min, and 2× SSC/0.05% Tween-20 (Tween-20, Sigma-Aldrich) three times for 5 min each cycle. Afterwards, cells were counterstained using 0.1 $\mu\text{g}/\text{ml}$, 4',6-diamidino-2-phenylindole (DAPI) (Sigma-Aldrich). Slides were rinsed with deionized distilled water (DDW) to remove excess DAPI and incubated in DDW for 2 min. Lastly, slides were mounted with Vectashield (Vector Laboratories, Burlington, Ontario, Canada).

TeloView: Semi-automated image acquisition and analysis

3D fluorescence microscopy was performed using a Zeiss AxioImager Z1 microscope (Carl Zeiss, Toronto, Ontario), equipped with an AxioCam HRm camera and 63×/1.4 oil Plan Apochromat objective as described previously [36]. The data acquisition was carried out using the AXIOVISION 4.8 software (Carl Zeiss). For 3D imaging, 80 image z-stacks were taken with a sampling distance of 200 nm along the z-axis and 102 nm in the x, y directions. Cyanine 3 (Cy3) and DAPI filters were used in multichannel mode in order to visualize the telomere PNA probe signals and nuclear DNA staining, respectively. To standardize fluorescent intensity between samples, the same exposure time of 800 ms was used for Cy3 imaging of telomeres in all interphase nuclei. Earlier work has shown that fluorescent intensity is proportional to size [37].

The recorded images were deconvolved using a constrained iterative algorithm [38], converted into TIFF files and analyzed using the TeloViewTM software [27] (3D Signatures Inc., Winnipeg, MB, Canada). TeloViewTM loads the 3D images and displays a maximum projection along the three axes, x, y, and z. Using TeloViewTM, we measured the following parameters for 30 interphase buccal cell nuclei per patient and determined telomeric signal

intensity (telomere length), the number of telomeric signals, the number of telomere aggregates, and a/c ratio. The latter pertains to the 3D spatial position of telomeres during the cell cycle and was described in detail by Vermolen et al. [27]: Telomeres in nuclei are positioned within a spheroid structure. A spheroid has the two main axes, a and b , which are equal in length, and a third axis c that has a different length; if $a < c$, we have a prolate spheroid; and if $a > c$, we have an oblate spheroid. We can therefore define a telomere ratio parameter, ρ_T , which gives us a measurement of the disk-like nature of this organization. If $\rho_T \sim 1$, then the telomeres are distributed in a spherical way within the cell. However, if $\rho_T > 1$, then the telomeric territory is more disk-like. This measurement has allowed us to classify the 3D telomere positions during the cell cycle. In brief, large a/c ratios represent cells in G2, while small a/c ratios represent cells in G0/G1 and S (for additional details, see [27]).

Using the different telomeric aspects described above, TeloView™ generated specific 3D telomere profiles for each buccal sample examined.

Statistical analysis

For each 3D parameter, by-pair analysis comparing each AD patient to his/her matched control was conducted via chi-square analysis or Wilcoxon rank sum tests. As a group of similar AD severity, the comparisons were done using randomized blocks analysis of variance and Mantel Haenszel stratified analysis, followed by the Breslow-Day test

for homogeneity across pairs as well as a log-linear analysis. To compare each AD severity to one another, we tested for severity effect with nested randomized block ANOVAs. Contingency analysis and Mantel-Haenszel stratified analysis were used to compare distributions of telomere signal fluorescent intensity (telomere length) categorized by quartiles. Significance level was set at $p < 0.05$. We calculated that with 44 matched pairs in a randomized block design we have more than 80% power to detect effect sizes as large as those observed previously between AD and controls of moderate and severe groups for both the telomere lengths and telomere signals.

RESULTS

Semi-automated 3D image acquisition and analysis using TeloView

3D imaging of buccal cells was performed from AD and non-AD study participants. Figure 1 shows a representative example of the 2D and 3D telomeric imaging that is performed on buccal cells (Materials and Methods). A comparison of all AD groups (mild, moderate, and severe) was published in our previous study [36]. The imaging data were quantified using TeloView™ (Materials and Methods).

When compared with our previous study [36], all 3D telomere parameters were confirmed as indicated in Table 2. Two exceptions were noted, namely, the a/c ratio and aggregate numbers in severe AD, which showed differences from the earlier study (Table 2,

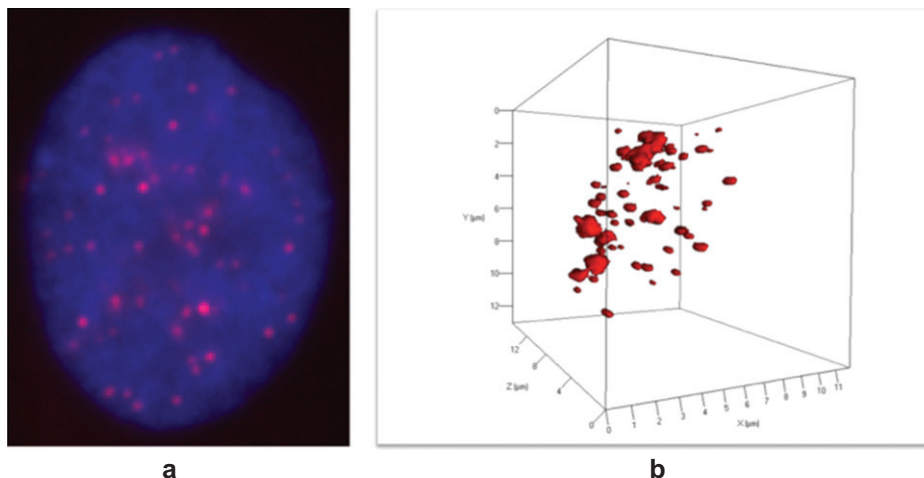


Fig. 1. Representative two (2)- and three dimensional (3D) image of a buccal cell nucleus hybridized with a CY3-labeled telomere probe (red) (Materials and Methods). (a) 2D image of nucleus hybridized with CY3-labeled telomere probe (red). Nucleus (blue). (b) 3D image of the identical nucleus. Telomeres are shown in red. Disease progression and telomere images were illustrated in [36].

Table 2
3D telomere parameters of AD and non-AD study participants

Participant	Diagnosis	Number of subjects	Nuclear 3D telomere parameters				
			Telomere length >15000 [a.u.]	Number of telomeres	Nuclear volume [μm^3]	<i>a/c</i> ratio	Telomeric aggregates
Mild AD	Mild AD	24	$p > 0.0001$	0.4487	0.1892	0.9807	0.2532
	Control	24					
Moderate AD	Moderate AD	15	$p > 0.0001$	0.0037	0.9863	0.1415	0.0554
	Control	15					
Severe AD	Severe AD	5	$p > 0.0001$	0.0452	0.9987	0.0024 [#]	0.1984 [#]
	Control	5					

Summary of 3D nuclear telomere parameters according to clinical diagnosis. While the data confirm the study cohort examined by Mathur et al. [36, Table 3], [#]indicates data different from the previous study. For the discussion of these data, see text. [a.u.] - arbitrary units.

$p = 0.0024$ and 0.1984 respectively). It is of note that the low number of severe AD participants and non-AD controls in the current cohort (five each) may likely be the cause of this difference (Tables 1 and 2).

We found a significant increase in telomere length attrition and telomere number elevation in buccal cells of AD patients compared to their respective controls and as AD progressed from mild to moderate to severe (Table 2). The telomere length differences measured between AD and non-AD and between mild, moderate and severe AD were highly significant (Table 2, $p < 0.0001$) as non-caregiver controls were participating in the current study. Moreover, the increase in the detected telomere numbers was significant as the disease progressed from mild to moderate to severe AD ($p = 0.0037$ for the difference between mild and moderate AD, and $p = 0.0452$ for the difference between moderate and severe AD).

As reported previously [36], nuclear volumes and *a/c* ratios remained unchanged ($p > 0.05$), with the exception of the *a/c* ratio in severe AD versus controls ($p = 0.0024$) (Table 2). Telomeric aggregates showed a trend to increase in moderate AD compared to mild AD and their respective controls ($p = 0.0554$) (Table 2).

DISCUSSION

While many studies have been performed the analysis of telomeres and genomic instability in AD [14–18], 3D analysis of telomeric architecture and DNA structure have not been conducted before, except as done in our previous study [36]. The current study was conducted under a new experimental design, in which we investigated age- and sex-matched non-caregiver controls and AD participants and the 3D telomeric parameters of buccal cells from both groups. This point is important as

caregivers are expected to exhibit telomere shortening as a result of constant and long-lasting daily stress [39, 40].

Nuclear volumes were unchanged and so were *a/c* ratios, except for severe AD. However, the low number of study participants in this group of AD patients may have had an impact on this result. An increase in telomere aggregates was noted in our previous AD study cohort compared to controls, and as AD progressed. In the current study, moderate AD showed a trend to significance ($p = 0.0554$), while severe AD did not follow this trend.

The current cohort confirmed the previously published data on 3D nuclear telomere profiling of AD and non-AD [28] showing that 3D nuclear telomere numbers were elevated and telomere lengths decreased. Overall, the difference between telomere lengths in AD and non-AD was more significant in the current study cohort than in the Mathur et al. [36] cohort. While the 2014 data showed significance in telomere length decrease, the current data indicate indirectly that the shorter telomeres of caregivers reduced the significance between the groups in the previous cohort. Therefore, the recent data on telomere length decreases show higher significance than those in the previous one [28]. While both studies indicate significant telomere length decreases, the current study shows the highest significance in differences measured between AD and non-AD and between AD subgroups (mild, moderate, and severe) ($p < 0.0001$). A recent meta-analysis that focused on telomere length alone confirmed our findings of shorter telomeres in AD as a general feature of AD [19].

Taken together, our data indicate that 3D telomere profiles can differentiate between AD and non-AD and between AD severity groups. This finding may be important in determining the onset of AD as well as its progression and enable future personalized AD

patient management. Limitations of this study are the numbers of patients enrolled and the medical classification system used (MoCA and MMSE without additional clinical classification, absence of information on disease duration and comorbidities). Future validation of these findings in larger cohorts and with detailed clinical classification is recommended.

ACKNOWLEDGMENTS

The authors would like to thank all study participants. We thank 3D Signatures Inc. for the use of TeloView™. The study was funded by the Cognition Challenge (Johnson & Johnson Innovation) and supported by the Canadian Consulate in San Francisco. We thank Mary Cheang for statistical analysis and Paul-Émile Crevier, Harpreet Bhullar, and Rosa Seo for technical support.

Authors' disclosures available online (<http://j-alz.com/manuscript-disclosures/16-1169r2>).

REFERENCES

- [1] Alzheimer's Association (2014) 2014 Alzheimer's Disease Facts and Figures. *Alzheimers Dement* **10**, e47-e92.
- [2] Hebert L, Weuve J, Scherr P, Evans D (2013) Alzheimer disease in the United States (2010-2050) estimated using the 2010 Census. *Neurology* **80**, 1778-1783.
- [3] McKhann G, Drachman D, Folstein M, Katzman R, Price D, Stadlan EM (1984) Clinical diagnosis of Alzheimer's disease: Report of the NINCDS-ADRDA Work Group under the auspices of Department of Health and Human Services Task Force on Alzheimer's Disease. *Neurology* **34**, 939-944.
- [4] Jack CR, Albert MS, Knopman DS, McKhann GM, Sperling RA, Carrillo MC, Thies B, Phelps CH (2011) Introduction to the recommendations from the National Institute on Aging-Alzheimer's Association workgroups on diagnostic guidelines for Alzheimer's Disease. *Alzheimers Dement* **7**, 257-262.
- [5] Albert MS, DeKosky ST, Dickson D, Dubois B, Feldman HH, Fox NC, Gamst A, Holtzman DM, Jagust WJ, Petersen RC, Snyder PJ, Carrillo MC, Thies B, Phelps CH (2011) The diagnosis of mild cognitive impairment due to Alzheimer's disease: Recommendations from the National Institute on Aging-Alzheimer's Association workgroups on diagnostic guidelines for Alzheimer's disease. *Alzheimers Dement* **7**, 270-279.
- [6] McKhann GM, Knopman DS, Chertkow H, Hyman BT, Jack CR, Kawas CH, Klunk WE, Koroshetz WJ, Manly JJ, Mayeux R, Mohs RC, Morris JC, Rossor MN, Scheltens P, Carrillo MC, Thies B, Weintraub S, Phelps CH (2011) The diagnosis of dementia due to Alzheimer's disease: Recommendations from the National Institute on Aging - Alzheimer's Association workgroups on diagnostic guidelines for Alzheimer's disease. *Alzheimers Dement* **7**, 263-269.
- [7] Hanninen T, Hallikainen M, Tuomainen S, Vanhanen M, Soininen H (2002) Prevalence of mild cognitive impairment: A population-based study in elderly subjects. *Acta Neurol Scand* **106**, 148-154.
- [8] Petersen RC, Smith GE, Waring SC, Ivnik RJ, Tangalos EG, Kokmen E (1999) Mild cognitive impairment: Clinical characterization and outcome. *Arch Neurol* **56**, 303-308.
- [9] Tan L, Yu J, Liu Q, Tan M, Zhang W, Hu N, Wang Y, Sun L, Jiang T, Tan L (2014) Circulating miR-125b as a biomarker of Alzheimer's disease. *J Neurol Sci* **336**, 52-56.
- [10] Nasreddine ZS, Phillips NA, Bedirian V, Charbonneau S, Whitehead V, Collin I, Cummings JL, Chertkow H (1995) The Montreal Cognitive Assessment, MoCA: A brief screening tool for mild cognitive impairment. *J Am Geriatr Soc* **53**, 695-699.
- [11] Folstein MF, Folstein SE, McHugh PR (1975) "Mini-mental state". A practical method for grading the cognitive state of patients for the clinician. *J Psychiatr Res* **12**, 189-198.
- [12] McDowell I, Kristjansson B, Hill GB, Hebert R (1997) Community screening for dementia: The Mini Mental State Exam (MMSE) and Modified Mini-Mental State Exam (3MS) compared. *J Clin Epidemiol* **50**, 377-383.
- [13] Boustani M, Peterson B, Hanson L, Harris R, Lohr K (2003) Screening for dementia in primary care: A summary of the evidence for the U.S. Preventative Services task force. *Ann Intern Med* **138**, 927-937.
- [14] Cai Z, Yan L, Ratka A (2013) Telomere shortening and Alzheimer's disease. *Neuromol Med* **15**, 25-48.
- [15] Geller LN, Potter H (1999) Chromosome missegregation and trisomy 21 mosaicism in Alzheimer's disease. *Neurobiol Dis* **6**, 167-179.
- [16] Migliore L, Testa A, Scarpato R, Pavese N, Petrozzi L, Bonuccelli U (1997) Spontaneous and induced aneuploidy in peripheral blood lymphocytes of patients with Alzheimer's Disease. *Hum Genet* **101**, 299-305.
- [17] Thomas P, Fenech M (2008) Chromosome 17 and 21 aneuploidy in buccal cells is increased with ageing and in Alzheimer's disease. *Mutagenesis* **23**, 57-65.
- [18] Panossian LA, Porter VR, Valenzuela HF, Zhu X, Reback E, Masterman D, Cummings JL, Effros RB (2003) Telomere shortening in T cells correlates with Alzheimer's disease status. *Neurobiol Aging* **24**, 77-84.
- [19] Forero DA, González-Giraldo Y, López-Quintero C, Castro-Vega LJ, Barreto GE, Perry G (2016) Meta-analysis of telomere length in Alzheimer's disease. *J Gerontol A Biol Sci Med Sci* **71**, 1069-1073.
- [20] Watson JD (1972) Origin of concatemeric T7 DNA. *Nat New Biol* **239**, 197-201.
- [21] Olovnikov AM (1972) The immune response and the process of marginotomy in lymphoid cells. *Vestn Akad Nauk SSSR* **27**, 85-87.
- [22] Kruk PA, Rampino NJ, Bohr VA (1995) DNA damage and repair in telomeres: Relation to aging. *Proc Natl Acad Sci U S A* **92**, 258-262.
- [23] de Lange T (2005) Shelterin: The protein complex that shapes and safeguards human telomeres. *Genes Dev* **19**, 2100-2110.
- [24] Thomas P, O'Callaghan NJ, Fenech M (2008) Telomere length in white blood cells, buccal cells and brain tissue and its variation with ageing and Alzheimer's disease. *Mech Ageing Dev* **129**, 183-190.
- [25] Gadji M, Adebayo Awe J, Rodrigues P, Kumar R, Houston DS, Klewes L, Dièye TN, Rego EM, Passetto RF, de Oliveira FM, Mai S (2012) Profiling three-dimensional nuclear telomeric architecture of myelodysplastic syndromes and acute myeloid leukemia defines patient subgroups. *Clin Cancer Res* **18**, 3293-3304.

- [26] Knecht H, Kongruttanachok N, Sawan B, Brossard J, Prévost S, Turcotte E, Lichtensztejn Z, Lichtensztejn D, Mai S (2012) Three-dimensional telomere signatures of Hodgkin- and Reed-Sternberg cells at diagnosis identify patients with poor response to conventional chemotherapy. *Transl Oncol* **5**, 269-277.
- [27] Vermolen B, Garini Y, Mai S, Mougey V, Fest T, Chuang T, Chuang A, Wark L, Young I (2005) Characterizing the three-dimensional organization of telomeres. *Cytometry A* **67**, 144-150.
- [28] Hayflick L (1965) The limited *in vitro* lifetime of human diploid cell strains. *Exp Cell Res* **37**, 614-636.
- [29] Campisi J (2001) Cellular senescence as tumor-suppressor mechanism. *Trends Cell Biol* **11**, 27-31.
- [30] Raz V, Vermolen BJ, Garini Y, Onderwater JJ, Mommaas-Kienhuis MA, Koster AJ, Young IT, Tanke H, Dirks RW (2008) The nuclear lamina promotes telomere aggregation and centromere peripheral localization during senescence of human mesenchymal stem cells. *J Cell Sci* **121(Pt 24)**, 4018-4028.
- [31] Kim MJ, Kim MH, Kim SA, Chang JS (2008) Age-related deterioration of hematopoietic stem cells. *Int J Stem Cells* **1**, 55-63.
- [32] Patel PL, Suram A, Mirani N, Bischof O, Herbig U (2016) Derepression of hTERT gene expression promotes escape from oncogene-induced cellular senescence. *Proc Natl Acad Sci U S A* **113**, E5024-E5033.
- [33] Ishikawa N, Nakamura K, Izumiya-Shimomura N, Aida J, Matsuda Y, Arai T, Takubo K (2016) Changes of telomere status with aging: An update. *Geriatr Gerontol Int Suppl* **1**, 30-42.
- [34] Seimiya H (2015) Predicting risk at the end of the end: Telomere G-tail as a biomarker. *EBioMedicine* **2**, 804-805.
- [35] Mai S (2010) Initiation of telomere-mediated chromosomal rearrangements in cancer. *J Cell Biochem* **109**, 1095-1102.
- [36] Mathur S, Glogowska A, McAvoy E, Righolt C, Rutherford J, Willing C, Banik U, Ruthirakuhan M, Mai S, Garcia A (2014) Three-dimensional quantitative imaging of telomeres in buccal cells identifies mild, moderate, and severe Alzheimer's disease patients. *J Alzheimers Dis* **39**, 35-48.
- [37] Poon SS, Martens UM, Ward RK, Lansdorp PM (1999) Telomere length measurements using digital fluorescence microscopy. *Cytometry* **36**, 267-278.
- [38] Schaefer LH, Schuster D, Herz H (2001) Generalized approach for accelerated maximum likelihood based image restoration applied to three-dimensional fluorescence microscopy. *J Microsc* **204**, 99-107.
- [39] Damjanovic AK, Yang Y, Glaser R, Kiecolt-Glaser JK, Nguyen H, Laskowski B, Zou Y, Beversdorf DQ, Weng NP (2007) Accelerated telomere erosion is associated with a declining immune function of caregivers of Alzheimer's disease patients. *J Immunol* **179**, 4249-4254.
- [40] O'Donovan A, Tomiyama AJ, Lin J, Puterman E, Adler NE, Kemeny M, Wolkowitz OM, Blackburn EH, Epel ES (2012) Stress appraisals and cellular aging: A key role for anticipatory threat in the relationship between psychological stress and telomere length. *Brain Behav Immun* **26**, 573-579.